Acta Pharmacologica Sinica (2015) 36: 1487–1496
 1671-4083/15
www.nature.com/aps

Original Article

Sirt1 is involved in decreased bone formation in aged apolipoprotein E-deficient mice

Wei HONG[1, 2], Xiao-ya XU[3], Zhao-hui QIU[1], Jian-jun GAO[3], Zhan-ying WEI[4], Li ZHEN[5], Xiao-li ZHANG[6, *], Zhi-bing YE[6, *]

[1]Department of Geriatrics, Huadong Hospital, Research Center on Aging and Medicine, Fudan University, Shanghai 200040, China; [2]Department of Bone Metabolism, Shanghai Key Laboratory of Clinical Geriatric Medicine, Shanghai 200040, China; [3]Department of Bone Metabolism, Institute of Radiation Medicine, Fudan University, Shanghai 200032, China; [4]Department of Osteoporosis and Related Bone Disease, Shanghai 6th People's Hospital, Shanghai Jiao Tong University, Shanghai 200233, China; [5]Laboratory Animal Center, Zhongshan Hospital, Fudan University, Shanghai 200032, China; [6]Department of Nephrology, Huadong Hospital, Fudan University, Shanghai 200040, China

Aim: Apolipoprotein E (ApoE) plays an important role in the transport and metabolism of lipids. Recent studies show that bone mass is increased in young apoE$^{-/-}$ mice. In this study we investigated the bone phenotype and metabolism in aged apoE$^{-/-}$ mice.
Methods: Femurs and tibias were collected from 18- and 72-week-old apoE$^{-/-}$ mice and their age-matched wild-type (WT) littermates, and examined using micro-CT and histological analysis. Serum levels of total cholesterol, oxidized low-density lipoprotein (ox-LDL) and bone turnover markers were measured. Cultured bone mesenchymal stem cells (BMSCs) from tibias and femurs of 18-week-old apoE$^{-/-}$ mice were used in experiments *in vitro*. The expression levels of Sirt1 and Runx2 in bone tissue and BMSCs were measured using RT-PCR and Western blot analysis.
Results: Compared with age-matched WT littermates, young apoE$^{-/-}$ mice exhibited high bone mass with increased bone formation, accompanied by higher serum levels of bone turnover markers OCN and TRAP5b, and higher expression levels of Sirt1, Runx2, ALP and OCN in bone tissue. In contrast, aged apoE$^{-/-}$ mice showed reduced bone formation and lower bone mass relative to age-matched WT mice, accompanied by lower serum OCN levels, and markedly reduced expression levels of Sirt1, Runx2, ALP and OCN in bone tissue. After BMSCs were exposed to ox-LDL (20 μg/mL), the expression of Sirt1 and Runx2 proteins was significantly increased at 12 h, and then decreased at 72 h. Treatment with the Sirt1 inhibitor EX527 (10 μmol/L) suppressed the expression of Runx2, ALP and OCN in BMSCs.
Conclusion: In contrast to young apoE$^{-/-}$ mice, aged apoE$^{-/-}$ mice showe lower bone mass than age-matched WT mice. Long-lasting exposure to ox-LDL decreases the expression of Sirt1 and Runx2 in BMSCs, which may explain the decreased bone formation in aged apoE$^{-/-}$ mice.

Keywords: apolipoprotein E; apoE$^{-/-}$ mice; aging; bone formation; osteocalcin; TRAP5b; Runx2; Sirt1; oxidized low-density lipoprotein; EX527; bone mesenchymal stem cells

Acta Pharmacologica Sinica (2015) 36: 1487–1496; doi: 10.1038/aps.2015.95; published online 23 Nov 2015

Introduction

Apolipoprotein E (apoE) is a structural component of lipoproteins and is required for the plasma clearance of lipoproteins through binding with lipoprotein receptors. ApoE-deficient (apoE$^{-/-}$) mice exhibit severe hyperlipidemia and develop spontaneous atherosclerosis[1, 2]. Dyslipidemia and atherosclerosis can often co-exist with osteoporosis, and lipid-lowering agents have been shown to have positive effects on osteoporosis[3-7]. However, only a few studies have described the skeletal changes caused by ApoE deficiency. Some studies have reported that young and adult apoE$^{-/-}$ mice exhibit a high bone mass phenotype due to increased bone formation rates[8-10]. Indeed, these mice show increased bone mass compared to that in wild-type (WT) controls despite the potentially adverse effects of spontaneous hypercholesterolemia and atherosclerosis. An *in vitro* study has further found that ApoE is expressed in primary murine calvaria osteoblasts at late stages of differentiation[8]. Conversely, when fed a high-fat diet, ApoE-deficient mice show reduced bone formation by stimulating p53-mediated apoptosis of osteoblastic cells[11]. Another study has found that at 28 weeks of age, the total bone mineral den-

* To whom correspondence should be addressed.
E-mail yezb2013@163.com (Zhi-bing YE);
zhangxiaoli76@163.com (Xiao-li ZHANG)
Received 2015-06-20 Accepted 2015-09-15

sity (tBMD) of apoE$^{-/-}$ mice was significantly higher than that of WT mice, whereas at 40 weeks of age, there was no significant difference in tBMD between apoE$^{-/-}$ and WT mice[12]. These studies suggest that the skeletal phenotype of apoE$^{-/-}$ mice may be influenced by a variety of factors, including age, high-fat diet, and renal function. Therefore, it is necessary to study the bone phenotype and metabolism of aged apoE$^{-/-}$ mice.

ApoE gene isoforms are related to aging, longevity, and a number of age-related diseases, including atherogenesis and osteoporosis[13-19]. ApoE-deficient mice develop many premature degenerative changes linked to different ages[20], suggesting that ApoE-deficient mice may serve as a good model to study aging. Another important gene that is correlated with lifespan and age-related diseases belongs to the sirtuin family[21, 22]. Sirtuins are highly conserved NAD^+-dependent deacetylases that have been shown to regulate lifespan in lower organisms and to affect diseases related to aging in mammals[23, 24]. Studies have found that Sirt1 plays an important role in the pathogenesis of atherosclerosis[25, 26]. Sirt1 also plays a key role in osteoblast regulation[27] and mesenchymal stem cell differentiation[28]. One study has shown that endothelial cell-specific Sirt1 transgenic ApoE-knockout mice have fewer atherosclerotic lesions than apoE$^{-/-}$ controls. This finding suggests that the observed effects of ApoE knockout on aging might be related to the insufficient expression of Sirt1[29]. A recent study has reported that aged (2.2-year-old) mesenchymal stem cell (MSC)-specific Sirt1 knockout (MSCKO) mice show reduced cortical bone thickness and trabecular volume. Young mice, however, exhibit less-pronounced effects[30]. To date, no studies have described the levels of Sirt1 expression in the bone tissues of apoE$^{-/-}$ mice.

Therefore, in this study, we determined the skeletal phenotypes of aged apoE$^{-/-}$ mice using micro-computed tomography (micro-CT). To further analyze the possible mechanisms related to this phenotype, we evaluated Sirt1 expression in the bone tissues of apoE$^{-/-}$ mice and examined the role of Sirt1 in osteoblast differentiation from bone marrow-derived mesenchymal stem cells (BMSCs).

Materials and methods

Experimental animals

All animal studies were conducted with the approval of the Committee on Animal Resources at Huadong Hospital, Fudan University. Male apoE$^{-/-}$ mice on a C57Bl/6J background and their WT littermates were purchased from the Nanjing Biomedical Research Institute (Nanjing University, Nanjing, China) at 18 weeks of age. The mice were maintained in groups under a strict 12-h light/dark cycle in a temperature-controlled environment (25 °C) with free access to food and water. All animals were fed a standard mouse diet containing 20.50% protein, 4.68% fat, 1.23% calcium, and 0.91% phosphorus.

Micro-CT analysis

Femurs collected from apoE$^{-/-}$ mice and WT mice at 18 and 72 weeks of age were dissected, cleaned, fixed in 10% Millonig's formalin, and transferred to 100% ethanol. The femurs were then analyzed using a SkyScan-1176 micro-CT instrument (Bruker Corporation, Kontich, Belgium). Scans were performed using PANalytical's Microfocus Tube, with a 8.96-μmol/L voxel size, a 45 kV, 500 μA, and a 0.6° rotation step (180° angular range). For trabecular bone, micro-CT evaluation was performed on a 1-mm region of metaphyseal spongiosa in the distal femur. The regions were located 0.5 mm above the growth plate. The index included tissue bone mineral density (BMD) and directly measured bone volume fraction (BV/TV), thickness (Tb.Th), number (Tb.N), and separation (Tb.Sp). For cortical bone, measurements were performed on a 0.5-mm region of the mid-diaphysis of the femur. The index included total area (Tt.Ar), cortical area (Tt.Cr), thickness (Ct.Th), and porosity. NR Econ software Version 1.6 (Bruker Corporation) was used for the three-dimensional (3D) reconstruction and viewing of images.

Histological analysis

The tibias of each mouse were fixed for 1 d in 4% paraformaldehyde in phosphate-buffered saline (PBS) at 4 °C. Specimens were decalcified in 10% EDTA in 0.05 mol/L Tris buffer for 7 d at 4 °C until the bones were soft and flexible. The samples were then processed and embedded in paraffin. Sections were cut and stained with hematoxylin and eosin (H&E) and histochemically analyzed for alkaline phosphatase (ALP) activity using a BCIP/NBT Kit (Beyotime Biotechnology, Nanjing, China) and analyzed for tartrate-resistant acid phosphatase (TRAP) activity using a Leukocyte Acid Phosphatase Kit for TRAP staining (Sigma, St Louis, MO, USA). Sections were then counterstained with methyl green and mounted in Kaiser's glycerol jelly. Calculations were performed on a minimum of duplicate specimens from five mice in each group.

Serum bone turnover markers and biochemistry

Serum from each mouse was analyzed individually and in duplicate for the bone formation marker osteocalcin (OCN) using enzyme-linked immunosorbent assays (ELISAs) with a Mouse Osteocalcin EIA Kit (Immutopics International, San Clemente, CA, USA), and for the bone resorption marker tartrate-resistant acid phosphatase 5b (TRAP5b) using Mouse TRAP Assays (Immunodiagnostic Systems Inc, Boldon, UK) according to the manufacturer's instructions. The average values of duplicate measurements were obtained for each mouse. Serum total cholesterol (TC) was measured using a Hitachi 917 autoanalyzer (Tokyo, Japan), and serum oxidized low-density lipoprotein (ox-LDL) was measured using a mouse ox-LDL ELISA Kit (Uscn Life Science Inc, Wuhan, China).

Cell preparation and culture

BMSCs were obtained from apoE$^{-/-}$ mice and WT mice (male, 18 weeks old). The femurs and tibias were removed under aseptic conditions. After removal of the surrounding muscle and connective tissue, the ends of the bones were cut to expose the bone marrow cavity. The cavity was washed three times with PBS, and the bone marrow was injected with L-DMEM medium. The collected cells were directly inoculated in

culture in a bottle and allowed to attach for 3 d before the removal of non-adherent cells. When cells reached confluence, they were detached with 0.25% trypsin and scraped from the surface of the culture plate. The second generation of cells was seeded at 1×10^5 cells/well in a six-well culture plate and cultured in L-DMEM containing 10% fetal bovine serum (FBS). Some cells were cultured in experimental culture medium supplemented with 10 μmol/L EX-527 (Sigma) for 12 h and collected. Alternatively, cells were supplemented with 20 μg/mL ox-LDL (Peking Union-Biololgy Co Ltd, Beijing, China); ox-LDL was added every 24 h, and cells were collected at 12, 24, 48, or 72 h after ox-LDL was added.

Real-time reverse transcription polymerase chain reaction (RT-qPCR)

The total RNA was extracted from tissues and cultured cells using TRIzol reagent (Invitrogen, Carlsbad, CA, USA) according to the manufacturer's protocol. Total RNA was reverse transcribed to cDNA using a QuantiTect Rev Transcription Kit (Qiagen, Chatsworth, CA, USA). The number of cDNA molecules in the reverse-transcribed samples was determined by real-time PCR using a modified method with a QuantiTect SYBR Green PCR Kit (Qiagen) on an Mx3000P Real-Time PCR system (Stratagene, La Jolla, CA, USA) according to the manufacturer's instructions. The primers were obtained from SBSgene (www.sbsgene.com) with the following sequences: Sirt1, 5′-GCAGGTTGCAGGAATCCAA-3′ and 5′-GGCAAGATGCTGTTGCAAA-3′ (63 bp, XM_006514342.1); Runt-related transcription factor 2 (Runx2), 5′-TGTTCTCTGATCGCCTCAGTG-3′ and 5′-CCTGGGATCTGTAATCTGACTCT-3′ (146 bp, XM_006523545.1); ALP, 5′-CACGCGATGCAACACTCAGG-3′ and 5′-GCATGTCCCCGGGCTCAAAGA-3′ (479 bp, XM_ 006538500.1); osteocalcin (OCN), 5′-ACCCTGGCTGCGCTCTGTCTCT-3′ and 5′- GATGCGTTTGTAGGCGGTCTTCA-3′ (240 bp, NM_007541.3); and glyceraldehyde -3-phosphate dehydrogenase (GAPDH), 5′-AGCCTCGTCCCGTAGACA-3′ and 5′-CTCGCTCCTGGAAGATGG-3′ (255 bp, NM_008084.3). The conditions for PCR were 12.5 μL of SYBR Green I Master Mix, 0.25 μmol/L each of forward and reverse primer, and 2 μL of sample, and H_2O to a final volume of 25 μL. A melting curve was obtained at the end of each run to discriminate specific from nonspecific cDNA products. The cDNA content was normalized by subtracting the cycle number of the GAPDH gene expression from that of the target gene expression (ΔCt=Ct of target gene-Ct of GAPDH), and the gene expression level was calculated using the $2^{-(\Delta Ct)}$ method.

Western blot analysis

All samples were lysed using cell lysis buffer (Beyotime, Nanjing, China) plus a 1:100 volume of phenylmethanesulfonyl fluoride (100 mmol/L). Protein was then quantified using BCA protein assays (P0012; Beyotime) with bovine serum albumin (BSA) as a standard. Sodium dodecyl sulfate polyacrylamide gel electrophoresis (SDS-PAGE) sample loading buffer (P0015, Beyotime) was added to the protein samples, and samples were heated for 5 min in a boiling water bath. Aliquots of samples (40 μg) were then subjected to SDS-PAGE using 12% gels under reducing conditions and electroblotted onto polyvinylidene difluoride (PVDF) membranes (Ipvh00010; Millipore, Bedford, MA, USA). The membranes were blocked with 5% fat-free dry milk in TBST (0.1% Tween-20 and 0.1 mol/L NaCl in 0.1 mol/L Tris-HCl, pH 7.5) for 2 h at room temperature and then incubated overnight at 4 °C with the following primary antibodies: rabbit anti-Sirt1 (1:2000; Proteintech, Chicago, IL, USA); goat anti-Runx2 (1:1000; Santa Cruz Biotechnology, Santa Cruz, CA, USA); and mouse anti-GAPDH (1:10 000; Kangcheng, Shanghai, China). The membranes were then incubated with horseradish peroxidase-conjugated secondary antibodies (1:5000; Santa Cruz Biotechnology) at room temperature for 1 h, and proteins were detected by chemiluminescence (P0018; Beyotime). Each incubation step was followed by three washes (10 min each) with TBST. The protein bands were quantitatively analyzed using an image analysis system (QuantityOne software; Bio-Rad, Hercules, CA, USA).

Statistical analysis

The data are presented as the mean±standard deviation (SD). Statistical significance was determined using Student's *t*-tests or one-way analysis of variance (ANOVA) followed by Dunnett's test. Analyses were performed using SPSS 17.0 (Chicago, IL, USA), and differences with *P*-values less than 0.05 were considered significant.

Results

Detection of decreased bone volume in aged apoE$^{-/-}$ mice by micro-CT

First, we performed quantitative analyses of the bone phenotype using reconstruction of a micro-CT on the distal metaphyseal region of the femurs from male WT mice and apoE$^{-/-}$ mice that were 18 and 72 weeks of age (Figure 1). Relative to WT mice, femurs from 18-week-old apoE$^{-/-}$ mice exhibited a marked increase in trabecular BMD, BV/TV, and Tb.Th (+30.43%, +39.69%, and +30.68%, respectively; $P<0.05$; Figure 1A and 1C). No changes in cortical parameters were observed between the femurs of young WT and apoE$^{-/-}$ mice (Figure 1E and 1G). In contrast, in 72-week-old animals, the extent of total bone loss was much greater in apoE$^{-/-}$ mice. The trabecular BMD decreased significantly in apoE$^{-/-}$ mice compared with that in WT mice (-30.68%, $P<0.01$). This result was also accompanied by decreases in body weight ($P<0.05$), femur trabecular BV/TV (-48.19%, $P<0.01$), Tb.Th (-30.58%, $P<0.05$), and Tb.N (-60.02%, $P<0.01$; Figure 1B and 1D). Moreover, measurements of cortical bone from aged apoE$^{-/-}$ mice showed decreased cortical thickness (Ct.Th; -40.96%, $P<0.05$) and increased cortical porosity (+32.14%, $P<0.05$; Figure 1F and 1H).

Reduced bone formation in aged apoE$^{-/-}$ mice

To determine whether the differences in bone architecture were accompanied by corresponding changes in markers of bone formation and resorption, we performed histomorphometric analysis of tibias from 18- and 72-week-old WT

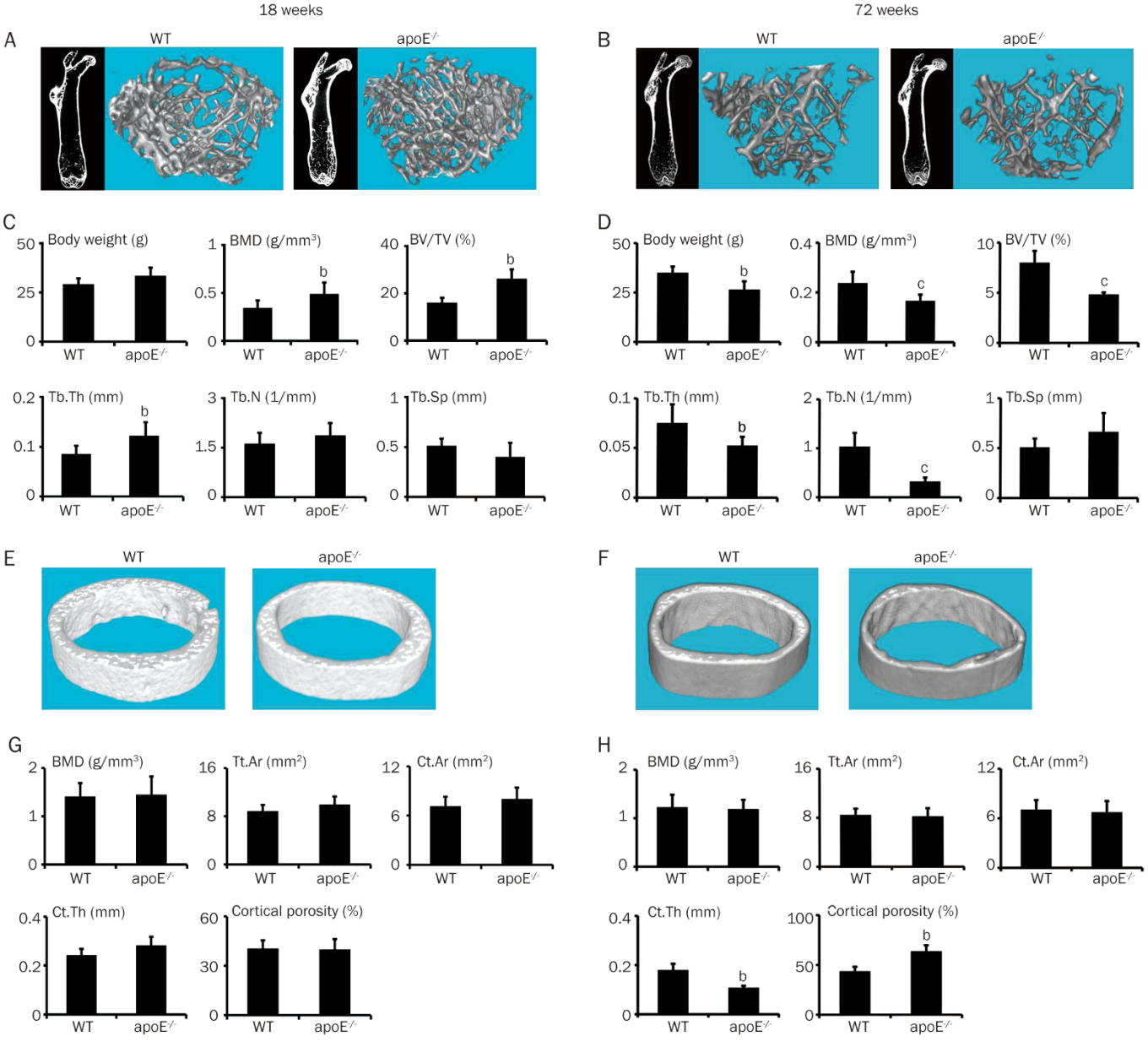

Figure 1. Bone mass in 18- and 72-week-old apoE$^{-/-}$ mice and their age-matched WT mice, as determined by micro-CT. (A and B) Representative 3D Micro-CT images showing regions of the trabecular bone in the distal femur. (C and D) Graphs represent measurements of total body weight, bone mineral density (BMD), trabecular bone volume (BV/TV), trabecular thickness (Tb.Th), trabecular number (Tb.N), and trabecular spacing (Tb.Sp) in the femurs. (E and F) Representative 3D micro-CT images showing regions of the cortical bone in the femurs. (G and H) Graphs represent measurements of bone mineral density (BMD), total area (Tt.Ar), cortical area (Ct.Ar), cortical thickness (Ct.Th), and cortical porosity. Statistical analysis was performed using a two-way ANOVA followed by a Dunnett's test. Mean±SD, n=7. ^{b}P<0.05, ^{c}P<0.01 *vs* WT.

and apoE$^{-/-}$ mice for markers associated with bone turnover (Figure 2). In 18-week-old mice, the results showed that the ratio of the ALP-positive osteoblast surface relative to the total bone surface (OB.S/BS) was increased (+28.70%, P<0.05) in apoE$^{-/-}$ mice compared with that in WT mice (Figure 2C). Somewhat contradictory to the results in the young apoE$^{-/-}$ mice, the ALP-positive area (OB.S/BS) decreased significantly in 72-week-old apoE$^{-/-}$ mice compared with that in WT mice (-40.7%, P<0.05; Figure 2D). No changes were observed in the osteoclast surface/bone surface (OC.S/BS) between the aged apoE$^{-/-}$ mice and WT mice at both young and old ages (Figure 2E and 2F). Consistently with results from previous studies, serum levels of OCN, a marker of bone formation, increased 1.22-fold in apoE$^{-/-}$ mice compared with that in WT mice at 18 weeks of age (P<0.05, Figure 3C). Serum levels of Trap5b also increased significantly (P<0.05, Figure 3D), whereas in 72-week-old animals, the serum levels of OCN were decreased relative to those of WT mice (-31.57%, P<0.05; Figure 3C).

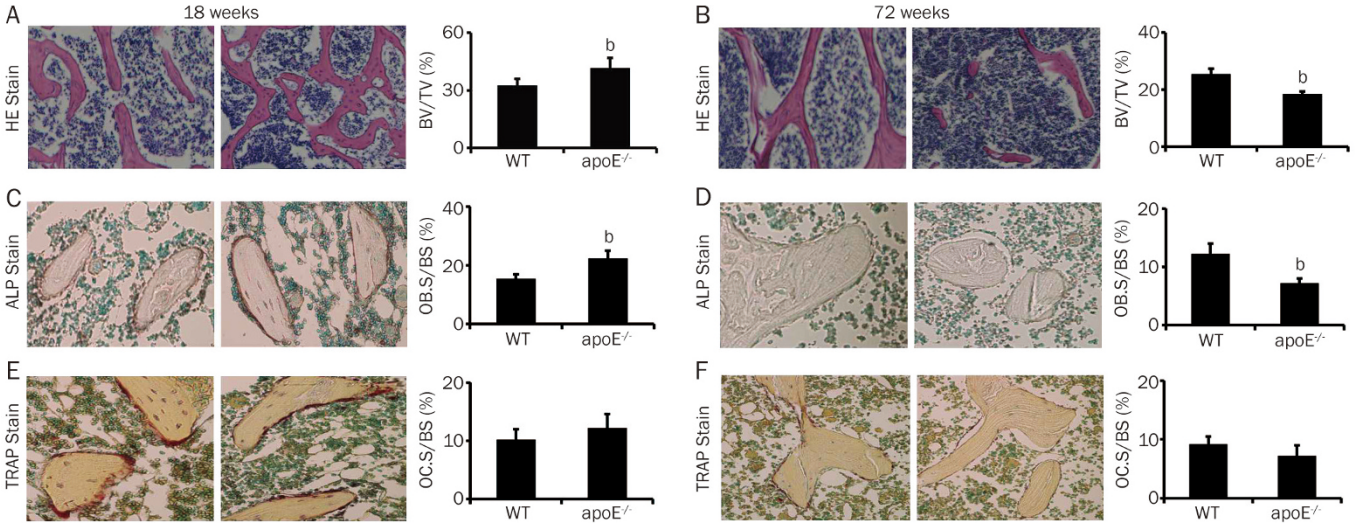

Figure 2. Changes of histochemistry in tibias of 18- and 72-week-old apoE$^{-/-}$ mice and their age-matched WT mice. (A and B) The H&E stained sections of trabecular bone in tibias. The trabecular bone volumes (BV/TV) were determined by histomorphometric analysis. Alkaline phosphatase (ALP) staining to quantify the osteoblast surface/bone surface (OB.S/BS) from 18-week-old (C) and 72-week-old (D) mice. The tartrate-resistant acid phosphatase (TRAP) staining of sections of trabecular bone in tibias from 18-week-old (E) and 72-week-old (F) mice to quantify the osteoclast surface/bone surface (OC.S/BS). Statistical analysis was performed using a two-way ANOVA followed by a Dunnett's test. Mean±SD, n=5. ^{b}P<0.05 *vs* WT.

However, the serum levels of Trap5b did not change significantly in aged apoE$^{-/-}$ mice relative to that in WT mice (Figure 3D). The serum levels of TC and ox-LDL were significantly higher in both 18-week- and 72-week-old apoE$^{-/-}$ mice compared with those in age-matched WT mice (P<0.01, Figure 3A and 3B).

Sirt1 expression decreased in bone tissues from aged apoE$^{-/-}$ mice

To further analyze the mechanisms mediating the rapid decrease in bone mass and bone formation in aged apoE$^{-/-}$ mice, we measured Sirt1 and Runx2 expression in bone tissue in both young and aged apoE$^{-/-}$ mice. In 18-week-old mice, *Sirt1* mRNA levels were 2.12-fold higher in apoE$^{-/-}$ mice than in WT mice (P<0.05). Similarly, the mRNA levels of the bone formation markers Runx2, ALP, and OCN were significantly higher in apoE$^{-/-}$ mice after normalization (2.9-, 1.29-, and 1.73-fold, respectively; P<0.05; Figure 4A). Western blot analysis confirmed these results (Figure 4C). However, in 72-week-old apoE$^{-/-}$ mice, protein and mRNA levels of Sirt1 and Runx2 in femurs were significantly decreased compared with those in age-matched WT animals (P<0.01, Figure 4B and 4D).

Ox-LDL induced a time-dependent decrease in Sirt1 expression during the osteogenic differentiation of BMSCs from apoE$^{-/-}$ mice *in vitro*

To further investigate whether Sirt1 plays an active role in the differentiation of BMSCs, we treated BMSCs from 18-week-old apoE$^{-/-}$ mice with the Sirt1 inhibitor EX527. After treatment with EX527 (10 μmol/L), the mRNA (Figure 5A) and protein levels (Figure 5B) of Runx2 decreased significantly (-23.57%, P<0.05 and -54.38%, P<0.01, respectively).

Ox-LDL was much higher in aged apoE$^{-/-}$ mice than in WT mice (Figure 3B); therefore, we examined whether Sirt1 was involved in the osteogenic differentiation of BMSCs during long-term exposure of apoE$^{-/-}$ mice to ox-LDL (Figure 6A and 6B). RT-PCR analysis showed that ox-LDL (20 μg/mL) enhanced the expression of *Sirt1* mRNA in BMSCs in the first 12 h (3.3-fold; P<0.05). However, after prolonged treatment with ox-LDL, the expression of *Sirt1* mRNA decreased at 72 h compared with that at 0 h (-48%; P<0.05), which indicated that the long-term effects of ox-LDL accumulation downregulated *Sirt1* expression in the BMSCs of apoE$^{-/-}$ mice. Similar results were observed for Runx2 mRNA and protein levels.

Discussion

In this study, we investigated the changes in bone phenotype and metabolism of aged apoE$^{-/-}$ mice to elucidate the mechanisms involved. Our results showed that aged apoE$^{-/-}$ mice had lower bone mass compared with age-matched WT mice. Moreover, continuous stimulation with ox-LDL decreased Sirt1 and Runx2 expression in BMSCs, providing insight into the mechanisms of reduced bone formation in aged apoE$^{-/-}$ mice.

We found that femur trabecular bone mass and BV/TV were higher in young apoE$^{-/-}$ mice than in WT mice. This was consistent with the results of most previous studies in which the mice were usually 3–8 months old[8-10]. However, in our study, the trabecular volume of aged apoE$^{-/-}$ mice decreased significantly compared with that of WT mice of the same age. Histological changes in the tibias further confirmed the decreased bone formation in aged apoE$^{-/-}$ mice. In addition, our *in vivo* study showed that Runx2 expression in bone tissue was decreased in aged apoE$^{-/-}$ mice compared with that in WT

mice. Runx2 is an early master transcription factor that initiates the transcriptional program for the osteogenic lineage; this leads to the upregulation of various bone-related genes and markers, such as OCN, a late bone-formation marker responsible for constructing the bone matrix[31, 32]. Interestingly, in our study, we found that serum OCN in aged apoE$^{-/-}$ mice decreased significantly, whereas the levels of the bone resorption marker Trap5b were not different between apoE$^{-/-}$ and WT mice. These results indicated that there were significant age-induced reductions in bone mass and the bone formation rate in aged apoE$^{-/-}$ mice. To the best of our knowledge, our present study is the first to report the bone phenotype and metabolism of aged apoE$^{-/-}$ mice. A similar study by Wang *et al* has found that although the trabecular BMD (tBMD) of femurs from 28-week-old apoE$^{-/-}$ mice was higher than that of WT mice, there was no significant difference in the tBMD between 40-week-old apoE$^{-/-}$ mice and WT mice. Moreover, the Tb.N and Tb.Th in trabecular bone increased with age and reached a peak at 28 weeks of age, after which these parameters decreased[12].

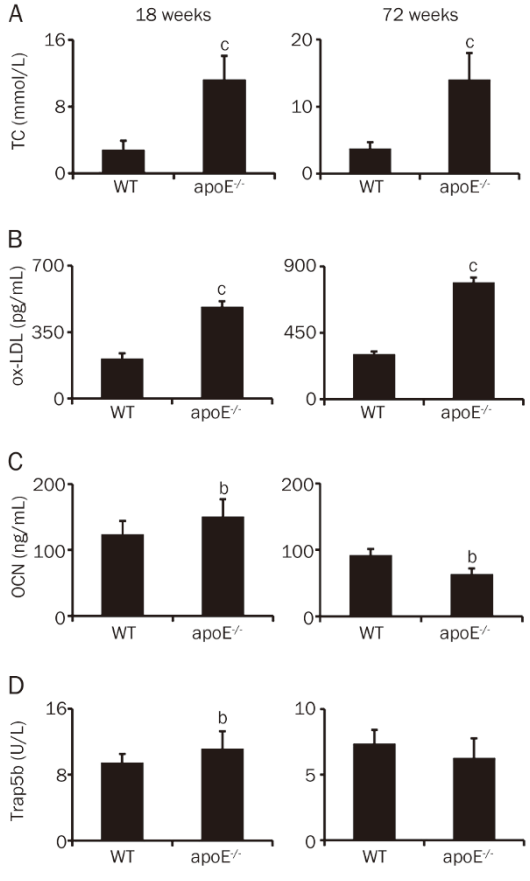

Figure 3. Serum biomarker and bone turnover marker levels in 18- and 72-week-old apoE$^{-/-}$ mice and their age-matched WT mice. Serum levels are shown for total cholesterol (TC, A), oxidized low-density lipoprotein (ox-LDL, B), bone formation marker osteocalcin (OCN, C) and bone resorption marker tartrate resistant acid phosphatase 5b (TRAP5b, D). Statistical analysis was performed using two-way ANOVA followed by Dunnett's test. Mean±SD, n=5. ^{b}P<0.05, ^{c}P<0.01, *vs* WT.

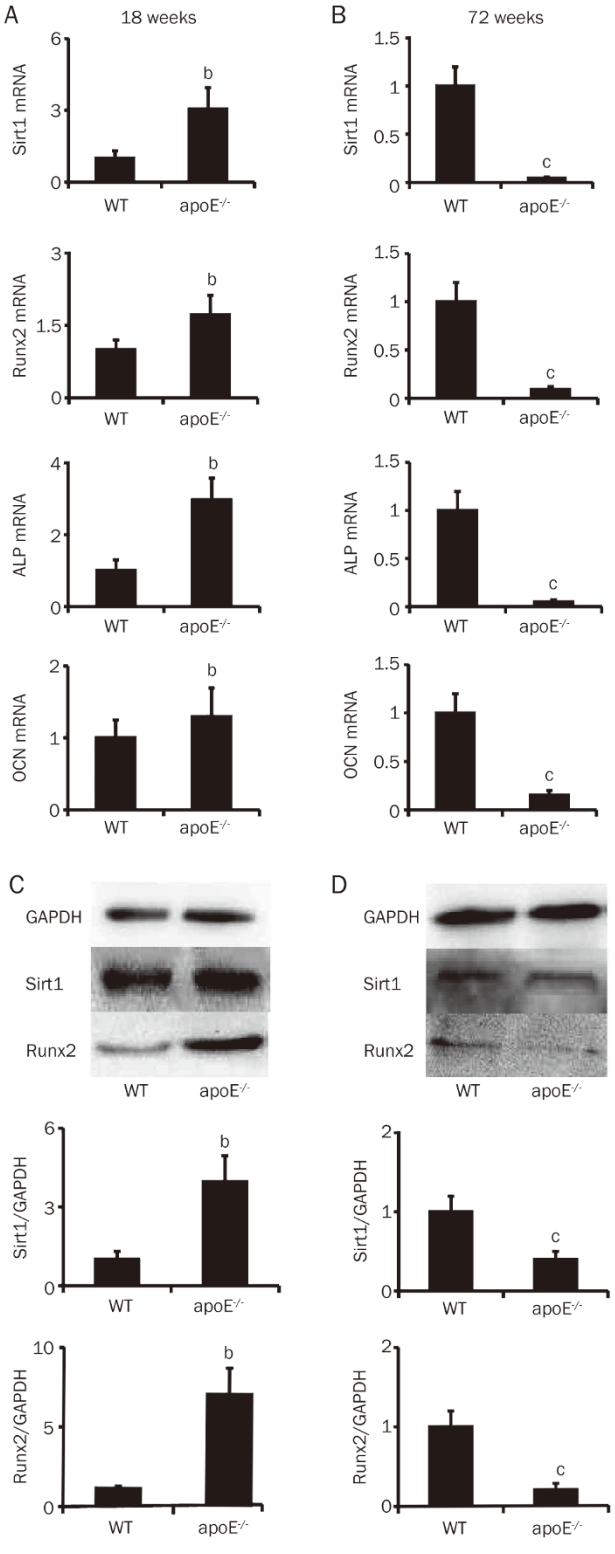

Figure 4. Sirt1 and relative expression of bone formation genes in 18- and 72-week-old apoE$^{-/-}$ mice and their age-matched WT mice. RT-PCR gene expression is shown for whole femurs of 18-week-old (A) and 72-week-old mice (B) for Sirt1, Runx2, ALP and OCN. Western blotting showing levels of Sirt1 and Runx2 in protein extracts from whole femur of 18-week-old (C) and 72-week-old mice (D). Statistical analysis was performed using a two-way ANOVA followed by a Dunnett's test. Mean±SD, n=4. ^{b}P<0.05, ^{c}P<0.01 *vs* WT.

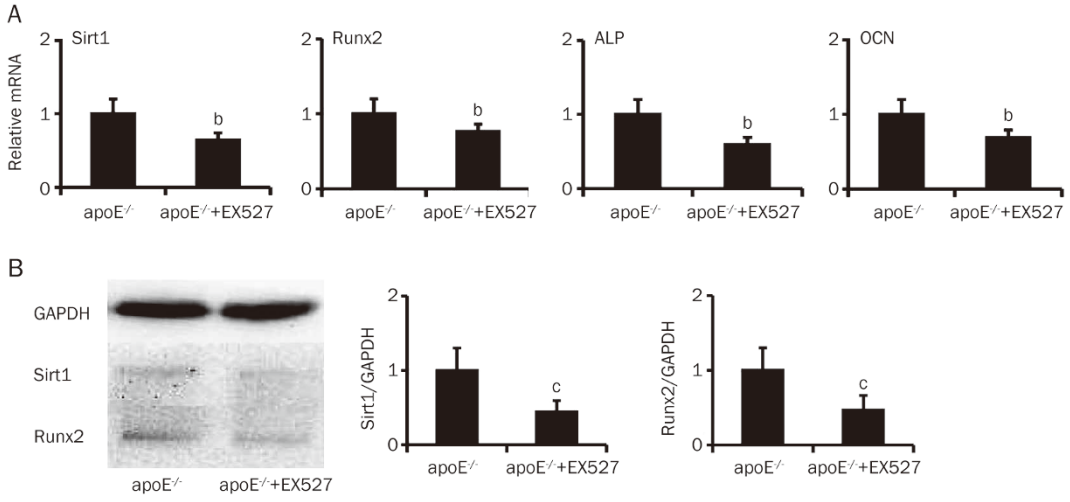

Figure 5. Sirt1 induced bone formation in the bone mesenchymal stem cells (BMSCs) from apoE$^{-/-}$mice *in vitro*. BMSCs from 18-week-old apoE$^{-/-}$ mice were cultured with 10 μmol/L EX-527 and the relative mRNA expression of Sirt1, Runx2, ALP and OCN (A) and protein (Western blotting) expression of Sirt1 and Runx2 (B) were analyzed for the mean change relative to an untreated control. Mean±SD, *n*=4. $^{b}P<0.05$, $^{c}P<0.01$ *vs* control.

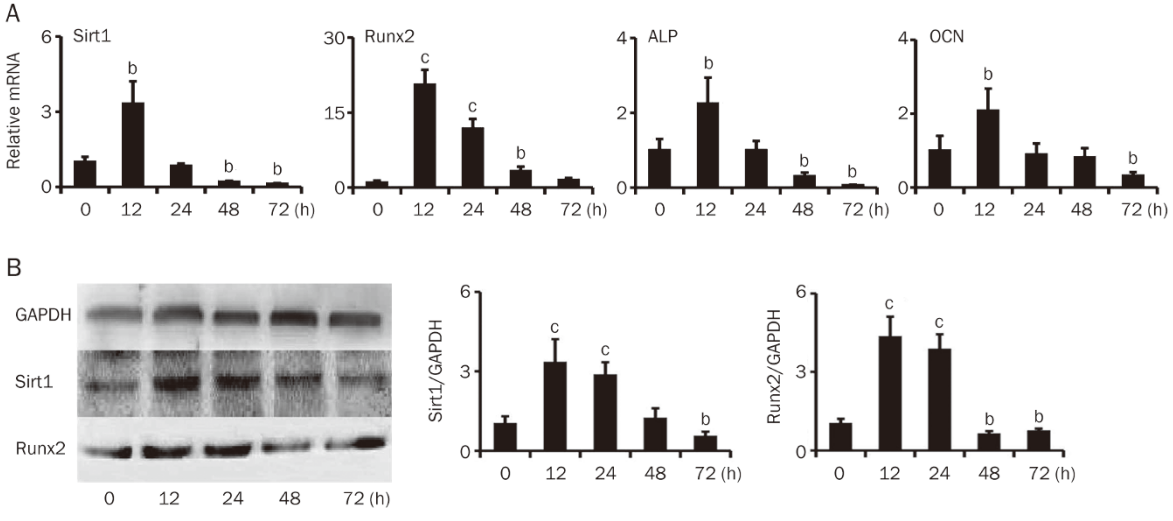

Figure 6. Ox-LDL induced a time-dependent decrease in Sirt1 expression during the osteogenic differentiation of BMSCs from apoE$^{-/-}$ mice *in vitro*. BMSCs from 18-week-old apoE$^{-/-}$mice were treated with ox-LDL (20 μg/mL). The relative mRNA expression of Sirt1, Runx2, ALP and OCN (A) and protein levels of Sirt1 and Runx2 (Western blotting, B) in BMSCs after exposure to ox-LDL for 0, 12, 24, 48, and 72 h. Mean±SD, *n*=4. $^{b}P<0.05$, $^{c}P<0.01$ *vs* 0 h.

Previous studies have found that ApoE is expressed in bone morphogenetic protein-2 (BMP-2)-treated mesenchymal progenitors and in mineralized primary osteoblast cultures[33]. ApoE can enhance the uptake of vitamin K-containing chylomicron remnants by human osteoblasts[34]. Moreover, although ApoE knockout itself directly affects osteogenic lineage cells and promotes bone formation *in vitro*[9, 33, 34], the final bone phenotype is the result of the combined effects of multiple factors. At a young age, the effects of ApoE deficiency on bones may play a more dominant positive role compared with the negative effects of hyperlipidemia and spontaneous atherosclerosis. However, in animals consuming a high-fat diet, ApoE deficiency has been shown to reduce bone formation through stimulation of p53-mediated apoptosis[11]. During aging, apoE$^{-/-}$ mice exhibited an accumulation of ox-LDL, accelerated atherosclerosis, increased production of reactive oxygen species, and enhanced cell aging; these features may lead to aggravated bone loss. Hypercholesterolemia-induced oxidant stress could accelerate the aging of hematopoietic stem cells from apoE$^{-/-}$ mice[35]. Compared with young mice, aged apoE$^{-/-}$ mice exhibit higher production of reactive oxygen species, leading to DNA damage and apoptosis of bone marrow cells[36]. Therefore, it is not surprising that the aged apoE$^{-/-}$ mice in this study exhibited decreased bone volume in contrast to the high bone mass observed in young mice. Similar contradictory situations were also found in other organs in apoE$^{-/-}$ mice. Aortic rings isolated from both young (6 to 18-week-old) and adult (20 to 35-week-old) male and female apoE$^{-/-}$

mice fed a standard chow diet exhibit a preserved endothelial oxide synthase (NO)-dependent relaxation response to acetylcholine (ACh) compared with that of WT controls. However, aged apoE$^{-/-}$ mice (50–70 weeks old) also show significant endothelial dysfunction, as demonstrated by a reduced aortic relaxation response to ACh[37]. Furthermore, various bone phenotypes during different stages of aging in the same type of mouse have also been demonstrated in other gene-knockout animal models. For example, in young (2-month-old) MSCKO mice, the effects of Sirt1 loss on bone are less pronounced, affecting only trabecular thickness without changing overall bone volume. However, in aged (2.2-year-old) MSCKO mice, cortical bone thickness and trabecular BV/TV are reduced 25% and 23%, respectively, as a result of reduced numbers of osteoblasts and lower bone formation rates[30]. Lyer *et al*[38] have reported that the bone formation rate is 40% higher in Foxo1,-3-4$^{f/f}$ and Osx1-Cre mice than in WT mice at 7 weeks of age. However, at 24 months of age, there are no differences in bone formation rates between the two types of mice.

To further analyze the mechanisms mediating this rapid decrease in bone mass and bone formation in aged apoE$^{-/-}$ mice, we first measured Sirt1 expression in bone tissues in young and aged apoE$^{-/-}$ mice. Sirt1 is the founding member of a group of proteins that have been well studied in aging research[39, 40], and Sirt1 affects a variety of biological functions, including DNA repair, energy metabolism, tumor suppression, and mitochondrial homeostasis[41, 42]. In addition, transgenic mice with approximately 2-fold higher levels of global Sirt1 expression are protected against metabolic decline due to aging[43]. These mice are also protected against aging-induced bone loss[44]. Sirt1$^{+/-}$ heterozygous female mice exhibit reduced bone mass characterized by decreased bone formation and increased marrow apoptosis[45]. The functional association between apoE knockout and Sirt1 has rarely been studied, and existing studies have focused mainly on atherosclerosis. Sirt1 has been shown to be atheroprotective in apoE$^{-/-}$ mice[25, 46, 47], whereas genetic overexpression of Sirt1 in LDL receptor-deficient (Ldlr$^{-/-}$) mice enhances atherosclerosis[44]. Stein *et al* have reported that young hypercholesterolemic apoE$^{-/-}$ Sirt1$^{+/-}$ mice treated with lipopolysaccharide exhibit more pronounced endothelial expression of intercellular cell adhesion molecule-1 (ICAM-1) and vascular cell adhesion molecule-1 (VCAM-1) compared with apoE$^{-/-}$ Sirt1$^{+/+}$ mice, suggesting that endogenous Sirt1 reduces endothelial activation in apoE$^{-/-}$ mice[25]. However, the association between apoE knockout and Sirt1 expression in the bone has not been studied before. Unlike the results observed in the arteries, in this study, we found that the expression of Sirt1 mRNA and protein in the bones of young apoE$^{-/-}$ mice was higher than that in the bones of WT mice (see additional data in Figure 7), whereas in aged apoE$^{-/-}$ mice, the expression of Sirt1 decreased significantly compared with that of WT mice. As mentioned above, Sirt1 plays an important positive role in bone metabolism, and the decreased expression of Sirt1 was consistent with the decreased bone mass and reduced bone formation rate in aged apoE$^{-/-}$ mice.

Based on these findings, we hypothesize that Sirt1 may be involved in the age-induced bone loss observed in apoE$^{-/-}$ mice. To test this hypothesis in more detail, we measured the expression of Sirt1 and Runx2 in BMSCs after stimulation with ox-LDL *in vitro*. Ox-LDL generates reactive oxygen species (ROS), which accelerate the aging of BMSCs[48]. In our study, after an initial increase (in the first 12 h), Sirt1 protein and mRNA expression in BMSCs from apoE$^{-/-}$ mice decreased more rapidly and became even lower than that at 0 h. These data indicated that continuous incubation with ox-LDL downregulated Sirt1 expression in the BMSCs of the apoE$^{-/-}$ mice. A recent study examining the effects of Sirt1 on the efferocytosis of ox-LDL-induced apoptotic RAW264.7 cells (macrophages) has revealed that the expression levels of Sirt1 and autophagy marker proteins are increased at 24 h and then decreased at 48 h[49]. Moreover, inhibition of Sirt1 in EX527-treated BMSCs reduces the expression of Runx2, suggesting that Sirt1 is involved in bone osteogenic differentiation in mice. The Sirt1 agonist resveratrol regulates Sirt1/Runx2 expression, thereby promoting the osteogenic differentiation of BMSCs[50]. Resveratrol promotes the osteogenesis of human mesenchymal stem cells by upregulating Runx2 gene expression via the Sirt1/Foxo3a axis[51]. This may explain why aged apoE$^{-/-}$ mice exhibited reduced bone formation rates and bone mass.

Together, our data showed that aged apoE$^{-/-}$ mice exhibited low bone mass and low bone formation. Sirt1 may play an important role in age-induced bone loss in aged apoE$^{-/-}$ mice. However, the direct relationship between ApoE knockout and Sirt1 expression in bone is still unclear. Further studies are required to elucidate these mechanisms.

Conclusions

Aged apoE$^{-/-}$ mice had lower bone mass compared with age-matched WT mice. Long-term treatment with ox-LDL decreased the expression of Sirt1 in BMSCs; this mechanism contributed to the low bone formation observed in these mice.

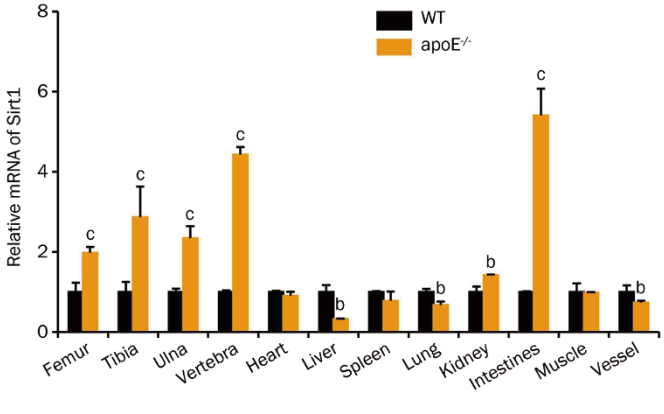

Figure 7. The mRNA expression of Sirt1 in different tissues from 18-week-old male apoE$^{-/-}$ mice and their age-matched WT mice. The mRNA expression of Sirt1 in the femur, tibia, ulna, vertebra, heart, liver, spleen, lung, kidney, intestines, muscle and vessels were analyzed for the mean fold change relative to controls. Mean±SD, n=4. ^{b}P<0.05, ^{c}P<0.01 *vs* WT.

Acknowledgements

The authors thank Prof Zhen-lin ZHANG (Department of Osteoporosis and Related Bone Disease, Shanghai 6th People's Hospital, Shanghai Jiao Tong University) for valuable advice regarding this study.

Author contribution

Zhi-bin YE designed the study; Xiao-li ZHANG directed the research; Wei HONG and Xiao-ya XU performed the histomorphometry, RT-PCR, and Western blotting; Zhan-ying WEI performed the micro-CT analysis; Zhao-hui QIU and Li ZHEN contributed to the animal experiments; Jian-jun GAO prepared the figures; Xiao-ya XU and Wei HONG analyzed the data; Wei HONG wrote the paper. All authors have read and approved the final paper.

References

1 Vasquez EC,Peotta VA,Gava AL, Pereira TM, Meyrelles SS. Cardiac and vascular phenotypes in the apolipoprotein E-deficient mouse. J Biomed Sci 2012; 19: 22.
2 Fazio S,Linton MF. Mouse models of hyperlipidemia and atherosclerosis. Front Bio sci 2001; 6: D515–25.
3 Trimpou P, Odén A, Simonsson T, Wilhelmsen L, Landin-Wilhelmsen K. High serum total cholesterol is a long-term cause of osteoporotic fracture. Osteoporos Int 2011; 22: 1615–20.
4 Marcovitz PA, Tran HH, Franklin BA, O'Neill WW, Yerkey M, Boura J, *et al*. Usefulness of bone mineral density to predict significant coronary artery disease. Am J Cardiol 2005; 96: 1059–63.
5 Schulz E, Arfai K, Liu X, Sayre J, Gilsanz V. Aortic calcification and the risk of osteoporosis and fractures. J Clin Endocrinol Metab 2004; 89: 4246–53.
6 Doherty TM, Fitzpatrick LA, Inoue D, Qiao JH, Fishbein MC, Detrano RC, *et al*. Molecular, endocrine, and genetic mechanisms of arterial calcification. Endocr Rev 2004; 25: 629–72.
7 Mundy G, Garrett R, Harris S, Chan J, Chen D, Rossini G, *et al*. Stimulation of bone formation *in vitro* and in rodents by statins. Science 1999; 286: 1946–9.
8 Bartelt A, Beil FT, Schinke T, Roeser K, Ruether W, Heeren J, *et al*. Apolipoprotein E-dependent inverse regulation of vertebral bone and adipose tissue mass in C57Bl/6 mice: modulation by diet-induced obesity. Bone 2010; 47: 736–45.
9 Schilling AF, Schinke T, Münch C, Gebauer M, Niemeier A, Priemel M, *et al*. Increased bone formation in mice lacking apolipoprotein E. J Bone Miner Res 2005; 20: 274–82.
10 Nikolov IG, Joki N, Nguyen-Khoa T, Ivanovski O, Phan O, Lacour B, *et al*. Chronic kidney disease bone and mineral disorder (CKD-MBD) in apolipoprotein E-deficient mice with chronic renal failure. Bone 2010; 47: 156–63.
11 Hirasawa H, Tanaka S, Sakai A, Tsutsui M, Shimokawa H, Miyata H, *et al*. ApoE gene deficiency enhances the reduction of bone formation induced by a high-fat diet through the stimulation of p53-mediated apoptosis in osteoblastic cells. J Bone Miner Res 2007; 22: 1020–30.
12 Wang M, Zhao LL, Li XP, Liao EY, Luo XH, *et al*. Changes in bone mineral density and microarchitecture with advancing age in the in male apolipoprotein E knockout mice. Chin J Endocrinol Metab 2010; 26: 406–10.
13 Shadyab AH, LaCroix AZ. Genetic factors associated with longevity: a review of recent findings. Ageing Res Rev 2015; 19: 1–7.
14 Seripa D, D'Onofrio G, Panza F, Cascavilla L, Masullo C, Pilotto A. The genetics of the human APOE polymorphism. Rejuvenation Res 2011; 14: 491–500.
15 Von Mühlen DG, Barrett-Connor E, Schneider DL, Morin PA, Parry P. Osteoporosis and apolipoprotein E genotype in older adults: the Rancho Bernardo study. Osteoporos Int 2001; 12: 332–5.
16 Pluijm SM, Dik MG, Jonker C, Deeg DJ, van Kamp GJ, *et al*. Effects of gender and age on the association of apolipoprotein E epsilon4 with bone mineral density, bone turnover and the risk of fractures in older people. Osteoporos Int 2002; 13: 701–9.
17 Dick IM, Devine A, Marangou A, Dhaliwal SS, Laws S, Martins RN, *et al*. Apolipoprotein E4 is associated with reduced calcaneal quantitative ultrasound measurements and bone mineral density in elderly women. Bone 2002; 31: 497–502.
18 Wong SY, Lau EM, Li M, Chung T, Sham A, Woo J. The prevalence of Apo E4 genotype and its relationship to bone mineral density in Hong Kong Chinese. J Bone Miner Metab 2005; 23: 261–5.
19 Peter I, Crosier MD, Yoshida M, Booth SL, Cupples LA, Dawson-Hughes B, *et al*. Associations of APOE gene polymorphisms with bone mineral density and fracture risk: a meta-analysis. Osteoporos Int 2011; 22: 1199–209.
20 Bonomini F, Filippini F, Hayek T, Aviram M, Keidar S, Rodella LF, *et al*. Apolipoprotein E and its role in aging and survival. Exp Gerontol 2010; 45: 149–57.
21 Dali-Youcef N, Lagouge M, Froelich S, Koehl C, Schoonjans K, Auwerx J. Sirtuins: the 'magnificent seven', function, metabolism and longevity. Ann Med 2007; 39: 335–45.
22 Kuningas M, Putters M, Westendorp RG, Slagboom PE, van Heemst D. SIRT1 gene, age-related diseases, and mortality: the Leiden 85-plus study. J Gerontol A Biol Sci Med Sci 2007; 62: 960–5.
23 Tissenbaum HA, Guarente L. Increased dosage of a sir-2 gene extends lifespan in *Caenorhabditis elegans*. Nature 2001; 410: 227–30.
24 Donmez G, Guarente L. Aging and disease: connections to sirtuins. Aging Cell, 2010; 9: 285–90.
25 Stein S, Lohmann C, Schäfer N, Hofmann J, Rohrer L, Besler C, *et al*. SIRT1 decreases Lox-1-mediated foam cell formation in atherogenesis. Eur Heart J 2010; 31: 2301–9.
26 Stein S, Schäfer N, Breitenstein A, Besler C, Winnik S, Lohmann C, *et al*. SIRT1 reduces endothelial activation without affecting vascular function in ApoE-/- mice. Aging (Albany NY) 2010; 2: 353–60.
27 Lee HW, Suh JH, Kim AY, Lee YS, Park SY, Kim JB. Histone deacetylase 1-mediated histone modification regulates osteoblast differentiation. Mol Endocrinol 2006; 20: 2432–43.
28 Bäckesjö CM, Li Y, Lindgren U, Haldosén LA. Activation of Sirt1 decreases adipocyte formation during osteoblast differentiation of mesenchymal stem cells. Cells Tissues Organs 2009; 189: 93–7.
29 Zhang QJ, Wang Z, Chen HZ, Zhou S, Zheng W, Liu G, *et al*. Endothelium-specific overexpression of class III deacetylase SIRT1 decreases atherosclerosis in apolipoprotein E-deficient mice. Cardiovasc Res 2008; 80: 191–9.
30 Simic P, Zainabadi K, Bell E, Sykes DB, Saez B, Lotinun S, *et al*. SIRT1 regulates differentiation of mesenchymal stem cells by deacetylating beta-catenin. EMBO Mol Med 2013; 5: 430–40.
31 Rosen CJ. Bone remodeling, energy metabolism, and the molecular clock. Cell Metab 2008; 7: 7–10.
32 Deschaseaux F, Sensébé L, Heymann D. Mechanisms of bone repair and regeneration. Trends Mol Med 2009; 15: 417–29.
33 Bächner D, Schröder D, Betat N, Ahrens M, Gross G. Apolipoprotein E (ApoE), a Bmp-2 (bone morphogenetic protein) upregulated gene in mesenchymal progenitors (C3H10T1/2), is highly expressed in murine embryonic development. Biofactors 1999; 9: 11–7.
34 Newman P, Bonello F, Wierzbicki AS, Lumb P, Savidge GF, Shearer MJ. The uptake of lipoprotein-borne phylloquinone (vitamin K1)

by osteoblasts and osteoblast-like cells: role of heparan sulfate proteoglycans and apolipoprotein E. J Bone Miner Res 2002; 17: 426–33.

35 Tie G, Messina KE, Yan J, Messina JA, Messina LM. Hypercholesterolemia induces oxidant stress that accelerates the ageing of hematopoietic stem cells. J Am Heart Assoc 2014, 3: e000241.

36 Tonini CL, Campagnaro BP, Louro LP, Pereira TM, Vasquez EC, Meyrelles SS. Effects of aging and hypercholesterolemia on oxidative stress and DNA damage in bone marrow mononuclear cells in apolipoprotein E-deficient mice. Int J Mol Sci 2013; 14: 3325–42.

37 Meyrelles SS, Peotta VA, Pereira TM, Vasquez EC. Endothelial dysfunction in the apolipoprotein E-deficient mouse: insights into the influence of diet, gender and aging. Lipids Health Dis 2011; 10: 211.

38 Iyer S, Ambrogini E, Bartell SM, Han L, Roberson PK, de Cabo R, *et al*. FOXOs attenuate bone formation by suppressing Wnt signaling. J Clin Invest 2013; 123: 3409–19.

39 Burnett C, Valentini S, Cabreiro F, Goss M, Somogyvári M, Piper MD, *et al*. Absence of effects of Sir2 overexpression on lifespan in *C*. elegans and *Drosophila*. Nature 2011; 477: 482–5.

40 Canto C, Auwerx J. Caloric restriction, SIRT1 and longevity. Trends Endocrinol Metab 2009; 20: 325–31.

41 Hasty, P. The impact energy metabolism and genome maintenance have on longevity and senescence: lessons from yeast to mammals. Mech Ageing Dev 2001; 122: 1651–62.

42 Simmons GE Jr, Pruitt WM, Pruitt K. Diverse roles of SIRT1 in cancer biology and lipid metabolism. Int J Mol Sci, 2015; 16: 950–65.

43 Banks AS, Kon N, Knight C, Matsumoto M, Gutiérrez-Juárez R, Rossetti L, *et al*. SirT1 gain of function increases energy efficiency and prevents diabetes in mice. Cell Metab 2008; 8: 333–41.

44 Herranz D, Muñoz-Martin M, Cañamero M, Mulero F, Martinez-Pastor B, Fernandez-Capetillo O, *et al*. Sirt1 improves healthy ageing and protects from metabolic syndrome-associated cancer. Nat Commun 2010; 1: 3.

45 Cohen-Kfir E, Artsi H, Levin A, Abramowitz E, Bajayo A, Gurt I, *et al*. Sirt1 is a regulator of bone mass and a repressor of Sost encoding for sclerostin, a bone formation inhibitor. Endocrinology 2011; 152: 4514–24.

46 Gorenne I, Kumar S, Gray K, Figg N, Yu H, Mercer J, *et al*. Vascular smooth muscle cell sirtuin 1 protects against DNA damage and inhibits atherosclerosis. Circulation 2013; 127: 386–96.

47 Qiang L, Lin HV, Kim-Muller JY, Welch CL, Gu W, Accili D. Proatherogenic abnormalities of lipid metabolism in SirT1 transgenic mice are mediated through Creb deacetylation. Cell Metab 2011; 14: 758–67.

48 Li X, Xiao Y, Cui Y, Tan T, Narasimhulu CA, Hao H, *et al*. Cell membrane damage is involved in the impaired survival of bone marrow stem cells by oxidized low-density lipoprotein. J Cell Mol Med 2014; 18: 2445–53.

49 Liu B, Zhang B, Guo R, Li S, Xu Y. Enhancement in efferocytosis of oxidized low-density lipoprotein-induced apoptotic RAW264.7 cells through Sirt1-mediated autophagy. Int J Mol Med 2014; 33: 523–33.

50 Shakibaei M, Shayan P, Busch F, Aldinger C, Buhrmann C, Lueders C, *et al*. Resveratrol mediated modulation of Sirt-1/Runx2 promotes osteogenic differentiation of mesenchymal stem cells: potential role of Runx2 deacetylation. PLoS One 2012; 7: 35712.

51 Tseng PC, Hou SM, Chen RJ, Peng HW, Hsieh CF, Kuo ML, *et al*. Resveratrol promotes osteogenesis of human mesenchymal stem cells by upregulating RUNX2 gene expression via the SIRT1/FOXO3A axis. J Bone Miner Res 2011; 26: 2552–63.